Influence of the aircraft crash induced local nonlinearities on the overall dynamic response of a RC structure through a parametric study

C Rouzaud, Fabrice Gatuingt, G Hervé, N Moussallam, Olivier Dorival

Influence of the aircraft crash induced local nonlinearities on the overall dynamic response of a RC structure through a parametric study

C. Rouzaud[1,2,3], F. Gatuingt[1], G. Hervé[2], N. Moussallam[3], O. Dorival[4,5]

[1]LMT (ENS Cachan, CNRS, Université Paris Saclay)
61 avenue du Président Wilson, 94235 Cachan, France

[2]Université Paris-Est, Institut de Recherche en Constructibilité, ESTP
28 avenue du Président Wilson, 94230 Cachan, France

[3]AREVA, 10 rue Juliette Récamier 69006 Lyon, France

[4]Icam, site de Toulouse, 75 avenue de Grande-Bretagne, 31076 Toulouse Cedex 3, France

[5]Université de Toulouse, Institut Clément Ader (ICA), INSA, UPS, Mines Albi, ISAE
135 avenue de Rangueil, 31077 Toulouse Cedex, France

Abstract

In the process of nuclear power plant design, the safety of structures is an important aspect. Civil engineering structures have to resist the accelerations induced by, for example, seismic loads or shaking loads resulting from the aircraft impact. This is even more important for the in-structures equipments that have also to be qualified against the vibrations generated by this kind of hazards. In the case of aircraft crash, as a large variety of scenarios has to be envisaged, it is necessary to use methods that are less CPU-time consuming and that consider appropriately the nonlinearities.

The analysis presented in this paper deals with the problem of the characterization of nonlinearities (damaged area, transmitted force) in the response of a structure subjected to an aircraft impact. The purpose of our study is part of the development of a new decoupled nonlinear and elastic way for calculating the shaking of structures following an aircraft impact which could be very numerically costly if studied with classical finite element methods. The aim is to identify which parameters control the dimensions of the nonlinear zone and so will have a direct impact on the induced vibrations.

In a design context, several load cases (and simulations) are analyzed in order to consider a wide range of impact (different loading surfaces, momentum) and data sets of the target (thickness, reinforcements). In this work, the nonlinear area generated by the impact is localized and studied through a parametric analysis associated with an sensitivity analysis to identify the boundaries between the elastic domain and this nonlinear area.

1. Introduction

Reinforced concrete structures are designed to withstand static and dynamic loads during their lifetime. Load durations of a few microseconds to milliseconds can be caused by explosions, airplane crashes, etc... When a structure is subjected to a brief mechanical shock, as it is the case when a projectile impacts a structure, several vibration regimes can be separated in terms of the appearance of the displacement field observed. Assuming that the structure is appropriately sized to withstand an aircraft impact, the determination of the shaking induced by the impact requires nonlinear dynamic studies on a significant time range after the shock. The response cannot be completely described using classical methods. The reason is that the finite element method associated with explicit integration time schemes would lead to prohibitive computation costs since the calculation must be carried out with a very refined mesh to represent all the transient dynamic response (ten linear elements per wavelength for good accuracy is usually assumed) that implies small time steps in the time integration scheme. As a consequence, the medium (between 10 and 100 wavelengths per substructure) and high (over 100 wavelengths per substructure) frequency ranges are often ignored in this type of simulation. One can also note that is impossible to simulate the response of a complete civil engineering structure with complex nonlinear behavior models [10, 18, 21, 5].

To solve the problem of shock induced vibrations in a reinforced concrete structure we developed a numerical strategy define in [20] that is presented in Figure 1.

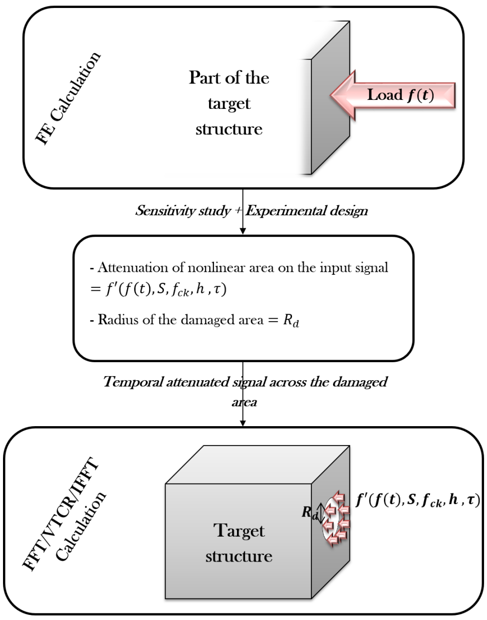

Figure 1: Global calculation strategy.

In this paper we will only focus on the first step of our strategy. The load is applied on a finite element model of the target structure and its response is calculated by a nonlinear Finite Element (F.E.) analysis. To simplify the problem we use a classical approach in which the aircraft is replaced by an equivalent force-time function. The loading diagram can be found using the Riera model [19, 2]. We can note that [11] shows the differences in terms of results in the frequency range simulated between a finite element aircraft model and its equivalent loading via the Riera method. The FE modeling of the aircraft generates a higher frequency content, mainly due to the folding effect of the aircraft fuselage. The Riera method is explained in details in [19].

Finally we use the current force calculated to determine the force-time history. Figure 2 shows the corresponding force-time history with an initial velocity of 120 m/s for the aircraft and a mass of 120 tons. In this figure, the impact force as a function of time, where the peak force is equal to 100 MN and the time duration of the force waveform is 350 ms, is normalized.

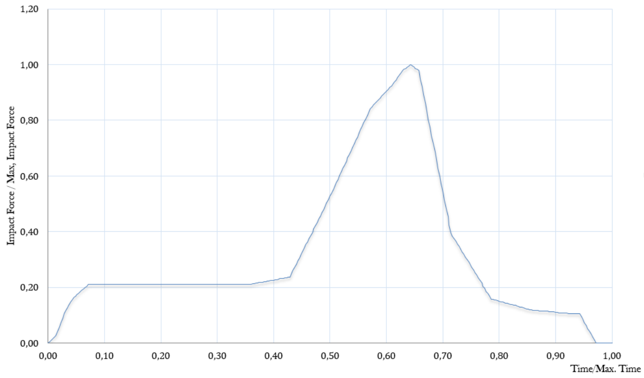

Figure 2: Force as a function of time (normalized).

According to the open literature, the evaluation of the type of impact generated in an aircraft crash leads us to consider the global impact as a soft shock [23]. Indeed if aircraft components produce individually different types of impact (elastic, inelastic, with rebound, hard, soft, ...), the global aspect could be classified as soft. The initial kinetic energy of the impacter can be decomposed after the impact into kinetic energy due to the possible rebound and energy dissipated during the impact. For a given kinetic energy, the energy dissipated during an impact is more important than the kinetic energy of rebound. The definition of soft shocks given in [8] and [4] is interesting because it is associated with a method of study of this type of impact (decoupling the calculation of force by the Riera formula and the calculation of the impacted structure). However it is a problem relative to the distinction from hard shocks. Indeed, comparing the movement of the target relative to the projectile is convenient because it induces a decoupling of the phenomena; it also corresponds to the intuitive definition of soft shock: a soft missile which hits a hard target. However this classification does not integrate well hard impacts when a rigid projectile going through a softer target or when the projectile impacts a flexible but tough target. There should be a criterion to distinguish not only soft and hard impacts on displacement or stiffness, but also on the threshold of fracture of materials; as suggests by [12]. Following this analysis, characterization of shock is "a priori" separated from the perforation. A soft shock, as well as a hard impact, can be both perforating or non-perforating ones. In the following we assume that the structure withstands the impact and as a consequence the perforating problem is eliminated.

The second step of our strategy, that was presented in a companion paper [20], is based on the application of the temporal attenuated signal obtained with the previous F.E. analysis at the boundary of the damaged area. This methodology will not be presented in thsi papaer.This damaged area corresponds in fact to an area around the impact surface where the damage is irreversible. In the case of a concrete slab, this area could be defined as a macro cracking zone. The response of the rest of the structure, which behavior remains linear, is computed with the Variational Theory of Complex Rays (VTCR) method in combination with a FFT/IFFT strategy. The VTCR is a wave-based computational approach dedicated to the resolution of forced vibration problems at a given frequency [13, 14].

In the strategy presented it is interesting to know more precisely the dimension of the nonlinear zone of the impact. Indeed restrict the geometry of finite element calculation to the damaged area is integrated in the strategy for calculating the induced vibrations (Figure 1) and also limits the significant numerical efforts required by this method. It is also important to surround the damaged area around the impact area because it is a zone of high energy dissipation and thus the determination of the vibrations induced in the structure is directly related to the transmission of energy through this area.

Based on the load function shown in Figure 2 we will investigate in this paper the influence of various parameters on the size of the nonlinear, or damaged, zone. These parameters are:

- the thickness of the target (h),
- the reinforcement ratio (longitudinal and shear rebars) (τ),
- the compressive strength of the concrete (f_{ck}),
- the loading surface (S),
- the momentum imposed.

The average tensile strength of concrete f_{ctm} is estimated in Eurocode 2 [7] by the following equations:

$$\begin{array}{ll} f_{ctm} = 0.30 f_{ck}^{2/3} & \text{if} f_{ck} \leq 50MPa \\ f_{ctm} = 2.12 ln(1 + \frac{f_{ck}+8}{10}) & \text{if} f_{ck} > 50MPa \end{array} \tag{1}$$

The impact of each parameter on the results will be explored using the Taguchi methods as defined in [24] and [22]. A parametric analysis associated with a sensitivity analysis allows us to determine the size of the damaged area and the attenuation of the nonlinear area on the input signal.

The paper is structured as follows: Section 2 presents the modeling choices and a simple parametric analysis (one-at-a-time strategy [6]) to define the ranges to be considered for the variables and then sensitivity analysis allows to account for combined effects; Section 3 illustrates a definition of sensitivity analysis and its application through the Taguchi method; Section 4 defines the empirical formulas derived from the sensitivity analysis application; finally, conclusions and perspectives are drawn in Section 5.

2. Using the parametric analysis to define the problem

Different impacts can be characterized and classified according to [12]. Nevertheless, this classification does not allow the prediction of the nonlinear damaged area of the impacted structure. Furthermore, this classification does not take into account the various input parameters of the target. In order to evaluate the influence of input parameters on this problem and to identify and eliminate the sets of parameters leading the perforation breakout of the target, we performed the following parametric study.

2.1. Modeling choices

In this work LS_Dyna [16] was used for the numerical simulations, with Lagrangian finite elements and explicit time integration. We decided to focus our study on a slab target with a square geometry of 40 $m \times 40$ m. The boundary conditions are defined as totally blocked (displacements and rotations) on each edge. A loading history corresponding to Figure 2 is taken into account, this force is applied over a period of 1 s. For a low computational cost the slab was modeled with a total of 40,000 uniform shell elements. To perform these FE calculations the element size should depend on the wavelength. Here we used ten element per wavelength as rule of thumb [1]. We consider a maximum frequency of 100 Hz in relation with the input force-time history. The entire slab is modeled and the mesh is the same for all tests. We used an explicit analysis and so the time step is affected by element size and material sound speed. In very rough terms, time step is proportional to $\frac{\text{element size}}{\text{soundspeed}}$. Material sound speed is proportional to $\frac{1}{\sqrt{\text{density}}}$.

The reinforced concrete has a complex behavior due to its heterogeneity, the complex behavior of the concrete and that of the concrete-reinforcement interface. The concrete is a nonlinear material with different behaviors in tension and compression, permanent strain with softening in compression and damage due to cracking in tension. Additionally in dynamics there is an increase of the elastic limit due to strain rate. To model the rupture of the material one can use the numerical technique of element erosion which is defined as the removal of finite elements according to a damage or stress state criterion. The steel reinforcement is also a nonlinear material (elastic-plastic), with a symmetric behavior in tension and compression. One should also consider a small dynamic effect due to the strain rate. Its failure will be considered when the total strain is large enough.

The material models used in the numerical simulations must represent as accurately as possible the behaviors described above. To do this with an acceptable computational cost, we used the nonlinear constitutive law of reinforced concrete *Mat_ Concrete_EC2* implemented in LS_Dyna [9]. LS-DYNA *Mat_ Concrete_EC2* model is for shell and Hughes-Liu beam elements only. It can represent reinforced concrete or plain concrete/plain reinforcement steel only. The position of the reinforcement steel cannot be explicitly defined within the concrete; hence the steel is evenly distributed, smeared, over the concrete cross section. The model includes concrete cracking in tension and crushing in compression, reinforcement yield, hardening and failure. Properties are thermally sensitive. Material data and equations governing the behavior (including thermal properties) are taken from [7]. Reinforcement is treated as separate sets of bars in the local element x and y axes. The concrete is assumed to crack in tension when the maximum in-plane principal stress (bending+membrane stress at an integration point) reaches tensile stress to cause cracking. Compressive behavior of the concrete initially follows the curve defined in Figure 3 as:

$$Stress = F_{cmax}\left(\frac{3\varepsilon}{\varepsilon_{c1}(2+(\frac{\varepsilon}{\varepsilon_{c1}})^3)}\right) \tag{2}$$

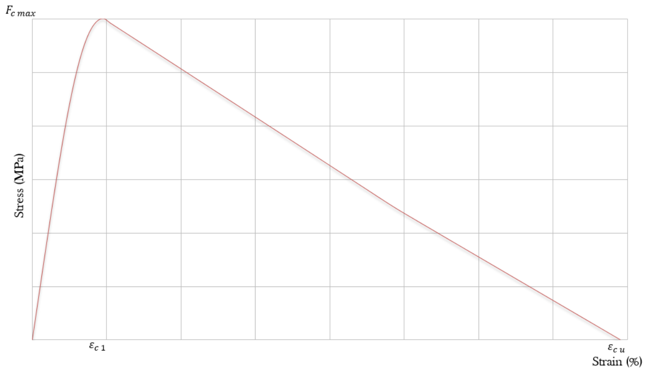

Figure 3: Mathematical model used in [7] to define the constitutive law of concrete.

where ε_{c1} is the strain corresponding to the ultimate compressive strength F_{cmax}, and ε is the current equivalent uniaxial compressive strain. The initial elastic modulus is given by $E = \frac{3}{2}\frac{F_{cmax}}{\varepsilon_{c1}}$. After reaching F_{cmax}, the stress decreases linearly with an increasing strain, reaching zero ε_{cu}. The strains ε_{c1} and ε_{cu} are by default taken from the Eurocode 2 or EC2 (abbreviations for BS EN 1992, Eurocode 2: Design of concrete structures) and are a function of temperature. At $20^{\circ}C$ they take values of 0.0025 and 0.02 respectively. F_{cmax} is also a function of temperature, given by the input compressive strength of concrete (which applies at $20^{\circ}C$) times a temperature-dependent softening factor taken from [7]. At $20^{\circ}C$ the behavior is elastic-perfectly-plastic, up to the onset of failure, after which the stress reduces linearly with increasing strain until final failure.

Figure 4 defines the EC2 tension-compression behaviour obtained from uniaxial compression and uniaxial tension quasi-static tests in displacements via a constant nodal velocity.

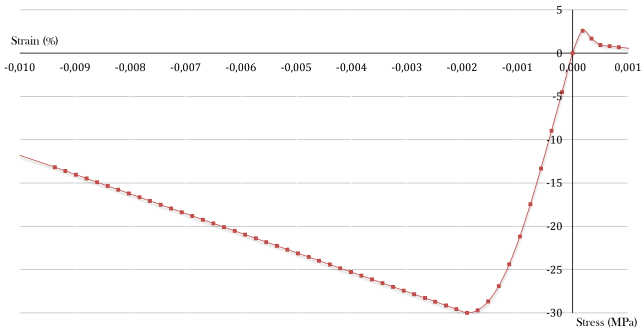

Figure 4: Stress / strain curves (tension-compression) of the EC2 law for concrete material.

2.2. Parametric analysis

As said earlier, the parametric analysis should allow us to determine the influence of the input parameters on the response of the structure. This study eliminates the values which lead to the perforation of the target. Indeed, according to open literature, an aircraft impact can be identified as a bending problem and not a punching one. Consequently we define four target parameters which could play an important role in the nonlinear response of the target. These parameters to be studied are the following:

- the loading surface of the aircraft impact,
- the characteristic strength of the concrete slab target,
- the reinforcement ratio,
- the thickness of the concrete slab.

In our approach and in the perspective to use it later in the Taguchi method, only one parameter changes from one simulation to the other.

We will in particular pay attention to the maximum deflection of the concrete slab, the radius of the damaged area which is numerically defined through the damage Mazars model [17], and reactions to boundary conditions in our simulation results. This damage model is a model simple, considered robust, based on the damage mechanics [15], which allow describe the reduction in the rigidity of the material under the effect of the creation of microscopic cracks in the concrete. It lean on only one scalar intern variable D, describing the isotropic damage of way, but distinguishing despite everything the damage from tension and the damage from compression. Please note that we chose to compare the response of the concrete slab with the elastic one (undamaged target). This comparison is done on the first oscillation cycle of the curve obtained.

2.2.1. Influence of the loading surface

In these simulations and for each loading surface configuration, the slab thickness was $1.2m$. and the concrete has a compressive strength of 40 MPa. For the reinforcement, 2 layers composed of $32mm$ steel reinforcing bars, $20cm$ spacing (noted as HA32@20 cm) in both directions were considered. Several loading surfaces are then studied: 4 m^2, 8 m^2, 12 m^2, 15 m^2, 18 m^2, 21 m^2, 37 m^2 and an average commercial aircraft surface (fuselage ($\phi = 3.76m \Rightarrow$ Surface $= 11m^2$) + wings ($L = 29m$)).

All surfaces over which the loading force (Figure 2) is applied have a circular form, except for the last one. For the average commercial aircraft we consider two areas: a disk for the fuselage and a rectangle for the wings. In this case, the loading history is a little bit different (see Figure 5).

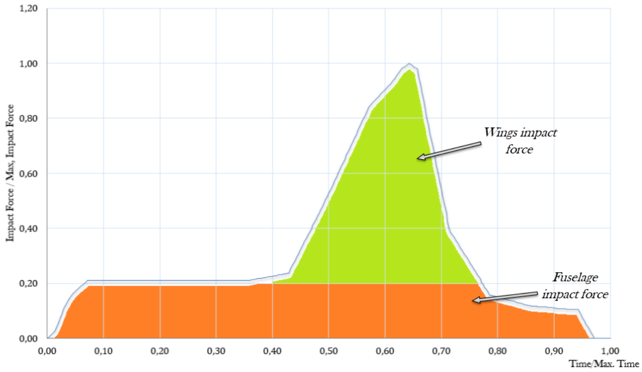

Figure 5: Loading history for an average commercial aircraft

Figures 6, 7 and 8 show the results obtained in terms of deflection of the slab, evolution of the damaged area and reaction force.

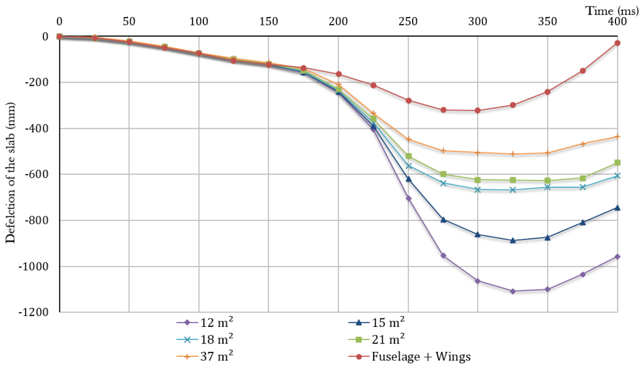

Figure 6: Evolution of the deflection of the slab for different load surfaces

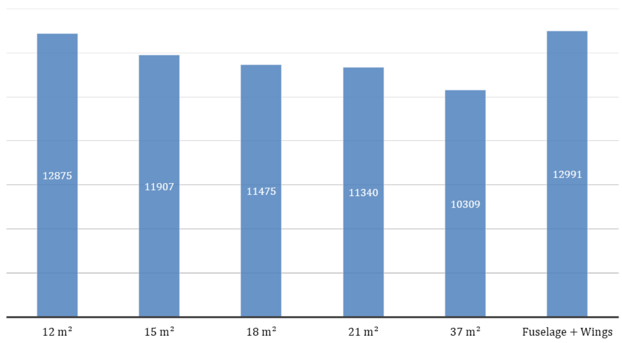

Figure 7: Evolution of the radius, in mm, of the damaged area for different load surfaces

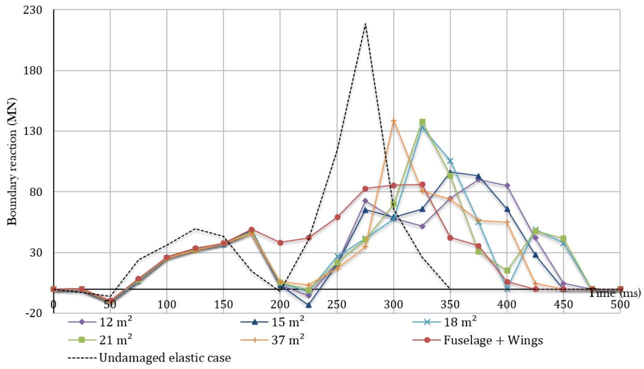

Figure 8: Evolution of the reaction force for different load surfaces

For the two smallest loading surfaces (4 m^2 and 8 m^2), we got an inversion of the Jacobian for some finite elements in the impact area leading to a simulation stop. Indeed, in both cases the elements undergo significant deformation that led to the perforation of the slab. The results of these two surfaces are then not considered in this study.

In Figure 6 the deflection of the slab decreases when the loading surface increases. The minimal deflection obtained (except for the aircraft) is 50 cm for S=37 m^2.

In Figure 7 the loading surface does not have a significant impact on the size of the nonlinear area. However, there is anyway a small decrease of the slab damage zone at the end of the simulation increasing the loading surface. The damaged area for the "Fuselage + Wing" is more important than can be explained by the size of the wings, and thus the dimension of the loading area.

In Figure 8 one can note a correlation between the boundary reaction and the slab damage area. Indeed the damage of the concrete slab dissipates some of the energy applied, hence a decrease in the force applied at the boundary conditions. One can also note that increasing the load surface provides a lower dissipation of energy at the boundary conditions. This directly translates into higher reaction force.

At the end for the simulations, the average radius of the damaged area is around $11m$ and the dissipation of the applied load through the nonlinear area is about 35 %.

In conclusion the load surface should be larger than the fuselage surface in order to avoid the perforation phenomenon for these slab dimensions. Finally, the results obtained for a loading surface that is more representative of an aircraft show a combination of the results for the various tested surfaces. For example the deflection of the slab is similar to teh one obtained for a very large load area and inversely the radius of the damaged area is close to that obtained for a small surface.

2.2.2. Influence of the concrete compressive strength

As in the previous subsection, in the simulations presented the slab thickness is 1.2 m and we used two layers of HA32@20 cm in both directions for the reinforcement. The load history (see Figure 2) is applied on a circular surface of 12 m^2. Several concrete compressive strength are now studied: 30 MPa, 40 MPa, 50 MPa and 60 MPa.

These values were chosen in order to represent ordinary and commonly used concretes. We can see the results in terms of deflection of the slab, boundary reaction force and radius of the damaged area in Figure 9, 10 and 11.

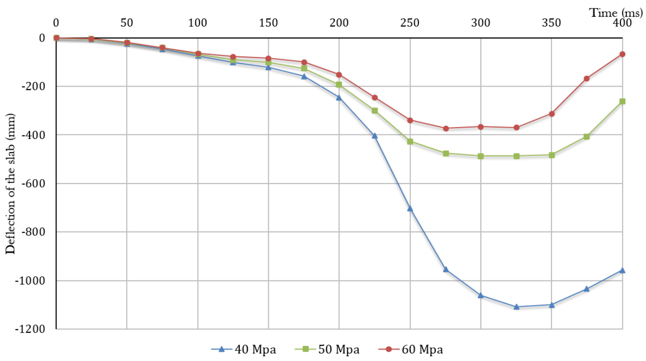

Figure 9: Evolution of the deflection of the slab for different concrete strengths

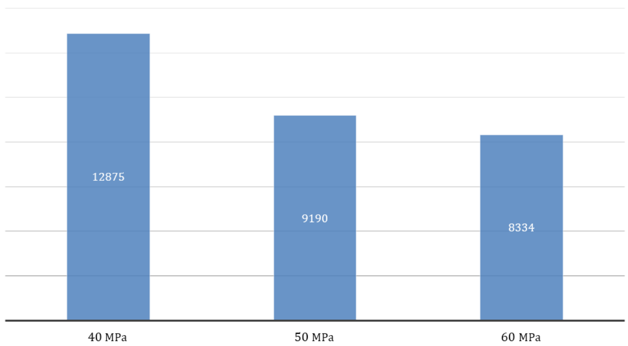

Figure 10: Evolution of the radius of the damaged area for various concrete strengths

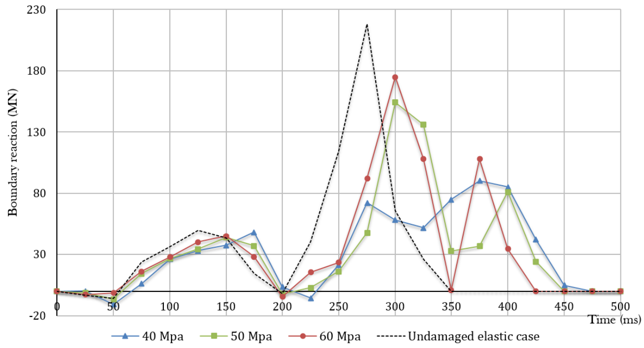

Figure 11: Evolution of the reaction force for various concrete strengths

As in the previous paragraph, we were not able to obtain results for all the configurations tested. For the smallest concrete strength (30 MPa) we got a perforation of the slab that is not wanted. Here we can note, quite logically, that increasing the concrete strength (and as a consequence the tensile strength) has an important effect. Nevertheless, the overall results seems to tend towards an asymptote from a resistance of 50 MPa. Indeed, beyond this resistance, one obtain an average deflection equal to 40 cm, a damaged radius around 8.5 m and a dissipation of the applied load through the nonlinear area about 22 %.

2.2.3. Influence of the reinforcement ratio

In the simulations presented the slab thickness is again 1.2 m and the concrete has a compressive strength of 40 MPa. The load history (see Figure 2) is also applied on a circular surface of 12 m^2. Four configurations of the reinforcement are then studied:

- HA25@25 cm (i.e. 0.2 $\%/m$ of steel) in both directions,
- HA25@20 cm (i.e 0.25 $\%/m$ of steel) in both directions,
- HA32@20 cm (i.e. 0.4 $\%/m$ of steel) in both directions,
- HA40@20 cm (i.e 0.63 $\%/m$ of steel) in both directions.

These four configurations were chosen because they are common in the civil engineering structures to which this study refers. The results obtained in terms of deflection of the slab, evolution of the damaged area and reaction force are shown in Figure 12, Figure 13 and Figure 14.

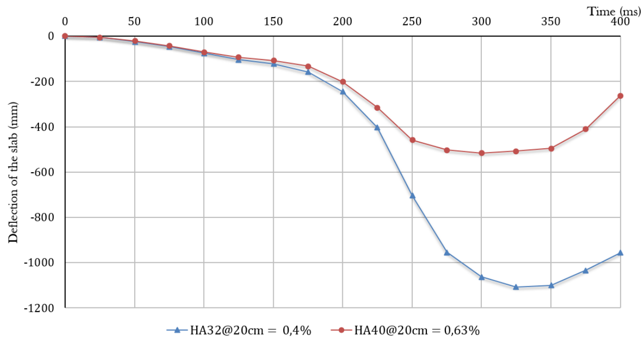

Figure 12: Evolution of the deflection of the slab for different reinforcements ratios

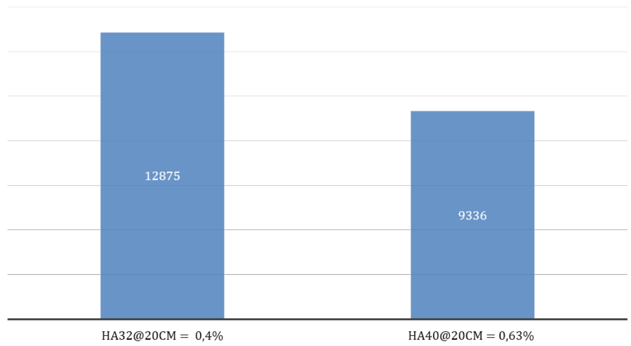

Figure 13: Evolution of the radius of damaged area for different reinforcements ratios

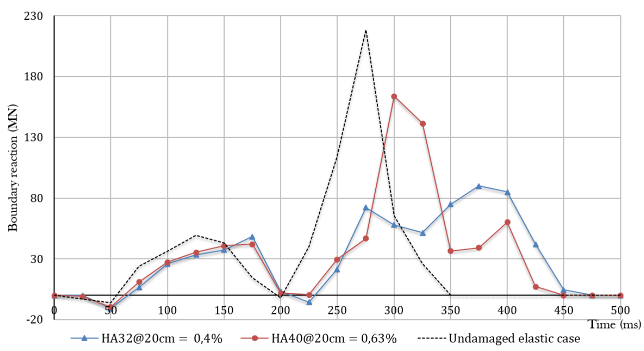

Figure 14: Evolution of the reaction force for different reinforcements ratios

The first two steel ratios are not relevant, because in both cases we get a perforation of the concrete slab. Only two configurations remain: HA32@20 cm and HA40@20 cm.

Figures 12, 13 and 14 show that we obtain an important difference in the results between these two configurations. We observe in Figure 12 that the deflection is reduced by a half; in Figure 13 that the damaged radius is reduced by more than 3 m and in Figure 14 that the maximum of the reaction force is multiplied by two. These results are in good agreement with the results of subsection 2.2.2. This shows that for a bending problem, the parameters which affect the flexural strength of the slab have a significant influence on the responses. However in the particular case of the reinforcement ratio, constructive arrangements put limits in terms of possible configurations. It would be difficult to design a slab with a reinforcement ratio higher than HA40@20 cm.

2.2.4. Influence of the slab thicknesses

In this subsection the slab thickness is the parameter. In the slab we impose two layers of HA32@20 cm in both directions for the reinforcement with a concrete compressive strength of 40 MPa. The load history (see Figure 2) is also applied on a circular surface of 12 m^2. Seven configurations of the thickness are then studied: 0.6 m, 0.9 m, 1.2 m, 1.35 m, 1.5 m, 1.8 m and 2.1 m.

The results are show in Figures 15, 16 and 17.

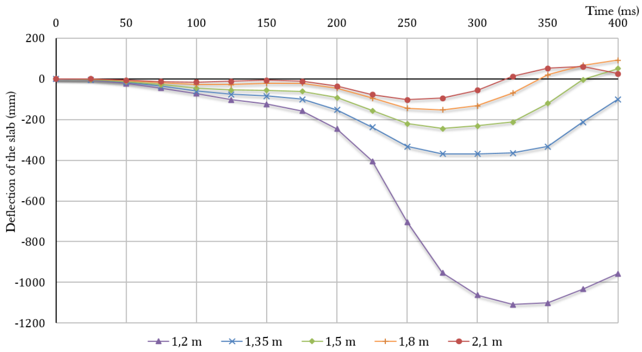

Figure 15: Evolution of the deflection of the slab with the slab thickness

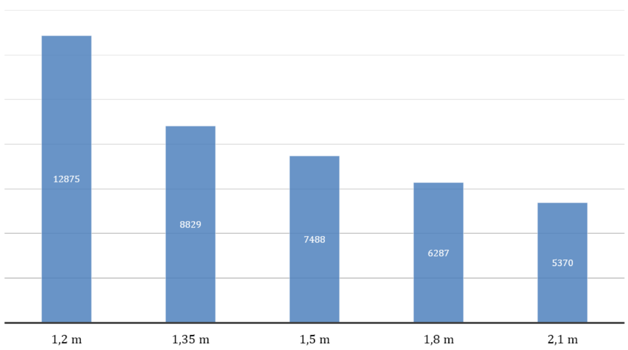

Figure 16: Evolution of the radius of damaged area with the slab thickness

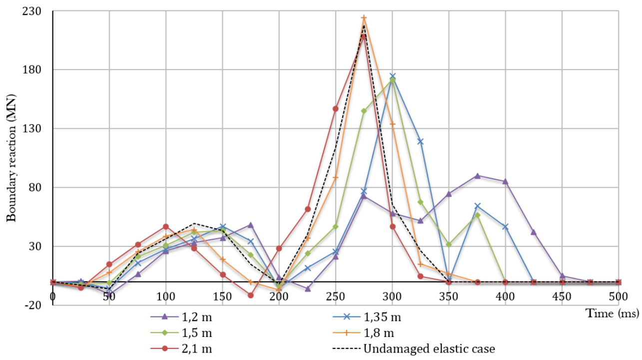

Figure 17: Evolution of the reaction force with the slab thickness

The first two thicknesses are not relevant, because in both cases we have a perforation of the concrete slab. These simulations are not considered hereinafter. In Figure 15 one can see that when increasing the thickness of the slab the maximum displacement will decrease. Moreover the slab will have a lower amplitude of vibrations and its residual displacement will approach zero. In this study, one can see that the results about the deflection and the nonlinear area decrease almost continuously. In Figure 16 one can observe that a thicker slab is less damaged and a reaction force approaching the elastic case (see Figure 17).

Here we can conclude that the thickness of the slab has a significant impact on the nonlinear area. In the cases studied, the results do not seem to converge towards a limit value.

2.2.5. Parametric analysis conclusion

As a conclusion to the parametric analysis, we can say that the minimum values leading to a perforation of the slab were determined. In this case, we did not pay particular attention to these configurations because the aircraft impact is treated – according to the state-of-the-art of the reinforced concrete structures we want to represent – as a flexural problem.

The results are in a good agreement with what could logically be expected if the dynamic load case is treated as a static problem. It is also difficult to identify a trend between the input parameters and the results and the interaction among parameters are impossible to perform in this way. The sensitivity analysis described in the next section is intended to fill this gap.

3. Using a sensitivity analysis by the Taguchi method

The aim of this section is to achieve a sensitivity study with a comparison between the effects of different parameters. It should allow us to identify which factors have an important effect on the maximum deflection of the concrete slab, on the radius of the damaged zone and on the reaction force at the supports.

3.1. Design of experiments concept

Sensitivity analysis or more precisely design of experiments, DOE, deals with planning, conducting, analyzing and interpreting controlled tests to evaluate the factors that control the value of a parameter or group of parameters. One also seek to acquire new knowledge by controlling one or more input parameters to obtain results validating a model with good economy (for example number of tests as low as possible). Indeed, this method is widely used in connection with the design of an industrial product. The problem of the designer is to find the "right" values of these parameters, i.e. the values for which the product will have the required behavior. So we need to identify the influence of parameters on the response of the product. The cost of a sensitivity study depends on the number and on the order of the different tests needed. Design of experiments is therefore to select and order tests to identify, at lower costs, the effects of parameters on the response of one product. This is a statistical method using simple mathematical concepts. Implementation of these methods involves four stages:

1) identify system parameters. These parameters correspond to physical quantities of the industrial product, which are allowed to change;

2) specify the values that you want to give them. On the actual product the parameters can evolve continuously (with an infinite number of possible values) or in a discrete manner;

3) define a sensitivity analysis, that is to say a series of tests to identify the model coefficients;

4) perform tests to identify the coefficients and conclude.

Design of experiments are defined in two categories: full and reduced plans:

- Full plans

This first category of sensitivity analysis intends to provide the most complete information possible on systems. The full plans are to test all possible combinations, varying all factors at all levels exhaustively.

- Reduced plans

In practice, full plans can only be used for systems with very few factors, or when each test is very simple and short. For example, in the case of a test with five parameters of three levels, it requires a full plan of $3^5 = 243$ tests... The objective of reduced plans is to select only few combinations of the varying parameters. They naturally reduce experimental or numerical costs but also reduce the available information on the system behavior. It is then necessary to ensure the relevance of the selection with the model to identify. Different techniques of reduced plans were defined [3, 24]. Among the most widely used and robust, let us mention the following two methods:

Box and Hunter method

The Box and Hunter method [3], could build reduced plans from full plans. It is intended only for models with two levels per parameter and is based on the following definition:

x_i and x_j are two parameters, each admitting two values, marked as $+1$ and -1. We define the level of interaction l_{ij} between x_i and x_j, the result of the product of their respective value. The level of interaction between these two parameters is therefore expressed formally if, in a given test, the two parameters proceed "in the same sense" or not. Table 1 shows the Box and Hunter table with 3 factors as an example.

Test	x_1	x_2	x_3	l_{12}	l_{13}	l_{23}	l_{123}
1	-1	-1	-1	$+1$	$+1$	$+1$	-1
2	$+1$	-1	-1	-1	-1	$+1$	$+1$
3	-1	$+1$	-1	-1	$+1$	-1	$+1$
4	$+1$	$+1$	-1	$+1$	-1	-1	-1
5	-1	-1	$+1$	$+1$	-1	-1	$+1$
6	$+1$	-1	$+1$	-1	$+1$	-1	-1
7	-1	$+1$	$+1$	-1	-1	$+1$	-1
8	$+1$	$+1$	$+1$	$+1$	$+1$	$+1$	$+1$

Table 1: Box and Hunter table with 3 factors

Taguchi method

Another well known technique of reduced plans is the Taguchi tables designed by the statistician Genichi Taguchi [24] in order to minimize the effect of uncertainties and measurement errors. In practice a Taguchi table is a table associated with one or more linear graph [25]. Table 2 shows the Taguchi table for seven parameters with two values (-1 and 1).

Test	x_1	x_2	x_3	x_4	x_5	x_6	x_7
1	-1	-1	-1	-1	-1	-1	-1
2	-1	-1	-1	1	1	1	1
3	-1	1	1	-1	-1	1	1
4	1	-1	-1	-1	-1	1	1
5	1	-1	1	-1	1	-1	1
6	1	-1	1	1	-1	1	-1
7	1	1	-1	-1	1	1	-1
8	1	1	-1	1	-1	-1	1

Table 2: Taguchi table L8 (2^7)

The sensitivity analysis, such as the methods mentioned it, directly gives the test sequence to achieve. Once those are completed, it remains to use the results to identify the model coefficients. To this aim we use statistical techniques based on an important property of experimental design: the orthogonality property. To identify the model coefficients, the idea is to use calculations of averages over sets of "balanced" results, i.e. orthogonal: this is the concept of effect. We thus define the (total) effect of a factor x_i at a level A_i as:

the average of results for which $x_i = A_i$ - the overall average.

It immediately follows from this definition that for each x_i factor, the sum of its effects at different levels is zero. Similarly, let us define the effect of the interaction between x_i and x_j at the levels A_i and A_j as:

the average of results for which $x_i = A_i$ and $x_j = A_j$
- x_i effect at level A_i
- x_j effect at level A_j
- the overall average.

The result is that for all factors x_i and x_j, the sum of the effects of their interaction with different levels of one or the other of the two factors is zero.

In conclusion, the design of experiments provides a simple and effective way to reduce the cost and increase the robustness of experimental studies in the design and validation of an industrial product. It allows the use of any product knowledge which the designer can have a priori, provides a framework for rigorous modeling, and its implementation requires only basic mathematical knowledge. In our approach, the choice of the methodologies used for sensitivity analysis could be discussed, in particular with respect to other approaches available for global sensitivity analysis. Let us mention two other methods. The Sobol indices adapted for probabilistic framework that is not our case. The Morris method is a one-step-at-a-time method (OAT) which implies that in each run only one input parameter is given a new value. This is more numerically costly than reduced plans methods.

3.2. Application of the Taguchi method to our study

As seen in the previous section, we have chosen to model an impacted reinforced concrete slab with shell elements using the *EC2_ Concrete* nonlinear behavior with LS_Dyna. The boundary conditions are defined as totally blocked (displacements and rotations) on each edges. The remaining parameters to vary are the following:

- loading surface: $S = 12; 15; 18; 21; 37m^2$,
- compressive strength : $f_{ck} = 40; 50; 60MPa$,
- slab thickness: $h = 1.2; 1.35; 1.5; 1.8; 2.1m$,
- reinforcement ratio: $\tau = 12.56; 15.71\%$,
- coefficient time: $c_t = 0.5; 1$,
- loading coefficient : $c_c = 0.5; 1$.

In the values to be taken into account, we removed those involving a perforation of the slab to overcome this kind of problem. We also added two other variables: c_t and c_c, a time coefficient, which could change the time duration of the force waveform, and a load factor respectively. The load factor could modify the peak force. These two values are factors which will allow us to observe the effect on the results of changing the momentum applied to the impacted slab. Table 3 relates the two extremum values considered for each parameter.

Levels	$S(m^2)$	$f_{ck}(MPa)$	$h(m)$	$\tau(\%)$	c_t	c_c
-1	12	40	1.2	12.56	0.5	0.5
1	37	60	2.1	15.71	1	1

Table 3: The sensitivity analysis levels

Using a reduced Taguchi sensitivity analysis with variables at two levels, allows us to reduce the number of tests to 8 instead of $2^6 = 64$ which leads to significant time savings in the numerical simulation. Table 4 shows the values taken by the simulations parameters for each test. For the numerical simulations we considered three important and representative results: the maximum deflection of the concrete slab, the radius of the damaged area and the maximum reaction force. These results are given in Table 5. As the reaction force is highly dependent on the applied load and as this applied load is different for the 8 tests, we have chosen to evaluate the maximum reaction force obtained compared to the maximum one in the elastic case (i.e. a slab which does not suffer any damage). This ratio gives an idea of the dissipation due to the nonlinear response of the slab.

Tests	S (m^2)	f_{ck} (MPa)	h (m)	τ %	c_t	c_c
1	12	40	1.2	12.56	0.5	0.5
2	12	40	1.2	15.71	1	1
3	12	60	2.1	12.56	0.5	1
4	12	60	2.1	15.71	1	0.5
5	37	40	2.1	12.56	1	0.5
6	37	40	2.1	15.71	0.5	1
7	37	60	1.2	12.56	1	1
8	37	60	1.2	15.71	0.5	0.5

Table 4: Lists of tests for the sensitivity analysis

Tests	Max. deflection (mm)	Damaged radius (mm)	Max. reaction (MN)	Max. reaction /Max. elas reaction (%)
1	-129	4380	123	95.2
2	-665	10441	134	61.4
3	-36.8	2261	159	72.8
4	-22.5	1130	84.8	77.7
5	-38.9	1696	82.8	75.8
6	-46.5	2615	190	87.0
7	-552	11441	117	53.6
8	-80.3	2559	94.5	73.1

Table 5: Numerical results for each test of the sensitivity analysis

Using the formula given in the previous section for the Taguchi tables, the effect at a level is defined by the average of all the results minus the overall average. From this, one can calculate the influence of each parameter on the three quantities of interest (deflection, damaged radius and reaction force). The results are reported in Table 6.

Variables	$S(m^2)$			$f_{ck}(MPa)$		
Levels	Max deflection (mm)	Damaged radius (mm)	Max. reaction /max. elas. reaction (%)	Max deflection (mm)	Damaged radius (mm)	Max. reaction /max. elas. reaction (%)
-1	-16.9	-12.4	2.1	-23.5	217.6	5.3
1	16.9	12.4	-2.1	23.5	-217.6	-5.3

Variables	$h(m)$			$\tau(\%)$		
Levels	Max deflection (mm)	Damaged radius (mm)	Max. reaction /max. elas. reaction (%)	Max deflection (mm)	Damaged radius (mm)	Max. reaction /max. elas. reaction (%)
-1	-160.2	2639.9	-3.8	7.2	379.2	-0.2
1	160.2	-2639.9	3.8	-7.2	-379.2	0.2
Variables	c_t			c_c		
Levels	Max deflection (mm)	Damaged radius (mm)	Max. reaction /max. elas. reaction (%)	Max deflection (mm)	Damaged radius (mm)	Max. reaction /max. elas. reaction (%)
-1	123.2	-1611.7	7.5	128.7	-2124.2	5.9
1	-123.2	1611.7	-7.5	-128.7	2124.2	-5.9

Table 6: Effect of each variable on the 3 quantities of interest

The influence of each parameter on each quantities of interest can then be compared (see Figure 18, 19, 20).

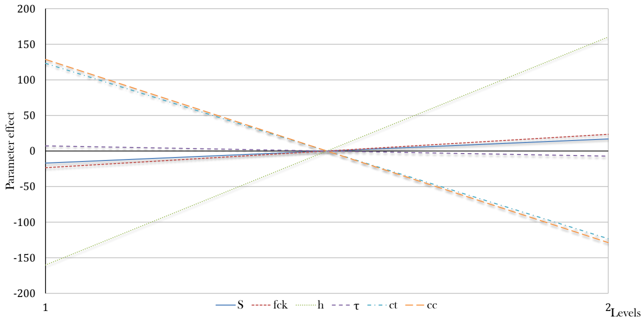

Figure 18: Influence of parameters on the deflection, in mm, of the concrete slab

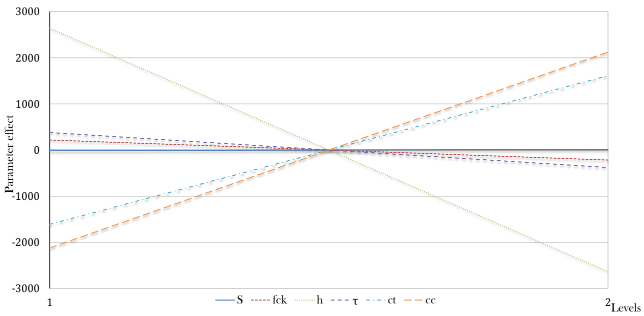

Figure 19: Influence of parameters on the radius, in mm, of the damaged area of the concrete slab

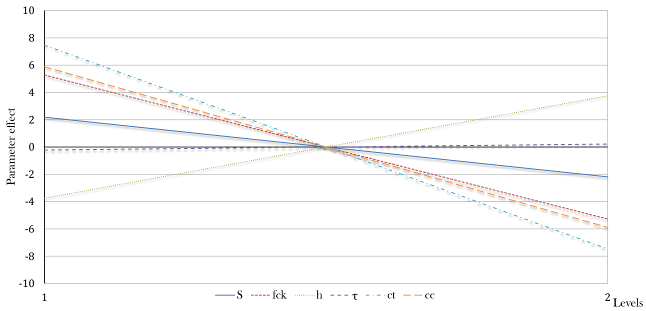

Figure 20: Influence of parameters on the maximum reaction, in MN, on boundary conditions of the slab concrete

This reduced sensitivity analysis gives the effect of each parameter on the quantities of interest. We can then conclude to a strong dependence of the overall results on the momentum of the load (c_t and c_c). We can also see that the thickness of the slab has a very important effect on the deflection of the slab and on the radius of the damaged area. Indeed, the stiffness of the impacted structure is directly linked to the thickness of the slab. In the case of the restitution to the boundaries of the load applied, the strength of the concrete and also the thickness of the slab both have a significant effect.

3.3. Sensitivity analysis conclusions

While a simple parameter study allows us to see only the influence of each variable separately, the realization of this sensitivity analysis associated with the Taguchi method allows us to compare the influence of each parameter on the results of the concrete slab. With this study we therefore prioritized these variables according to their importance on the nonlinear area. We can then conclude that firstly the momentum applied, secondly the thickness of the slab (Figures 18, 19) and thirdly the concrete strength (Figure 20) are the parameters which have the more influence.

However, the results obtained are highly dependent on the choice of the levels for each variable. For example increasing the difference between the two levels of a parameter could, at the same time, increase its effect on the response. So levels must be chosen in this scope. It is in this context that the previous parametric studies allow to estimate these values and make our analysis robust.

4. Determination of predictive empirical formulas

The aim of this section is to link all the results obtained in the previous sections. The determination of a formula would allow us to have a rough estimate of the different results (maximum deflection of the slab, damaged radius and reaction ratio) before introduction of a finite element calculation.

In our case, we will introduce one equation for each quantity of interest. We will use the following methodology:

- let A be the sought quantity: F, $r_{damaged}$ or $R_{max.\ force/max.\ elas.\ force}$,

- in the range of assigned variation we have six parameters: the thickness h of the slab, the loading surface S, the maximum strength of the concrete in compression f_{ck}, the ratio of the slab reinforcement τ and the momentum coefficients c_t and c_c.
- we then search for a simplified and empirical law as the following form:

$$A(h, S, f_{ck}, \tau, c_t, c_c) = \bar{A} + c_1^A.\hat{h} + c_2^A.\hat{S} + c_3^A.\hat{f_{ck}} + c_4^A.\hat{\tau} + c_5^A.\hat{c_t} + c_6^A.\hat{c_c} \quad (3)$$

where $c_1^A, c_2^A, c_3^A, c_4^A, c_5^A$ and c_6^A are constants associated to the quantity A which have to be determined from calculations of sensitivity analysis. In fact these constants determine the effect of each parameter. $\bar{A}$ is the average of the results considered A on all trials deducted from the Taguchi table. $\hat{p}$ corresponds to the normalized value of the parameter p defined as follows:

$$\hat{p} = \frac{(p - \bar{p})}{\sigma_p} \in [-1; 1] \Rightarrow \begin{cases} \hat{p}_{level\ -1} & = & -1 \\ \hat{p}_{level\ 1} & = & 1 \end{cases} \quad (4)$$

with $\bar{p}$ the average of parameter p between these two levels chosen and σ_p the standard deviation ($\sigma_p = -p_{level\ -1} + \bar{p} = p_{level\ 1} - \bar{p}$).

For three sought quantities, the following formulas are obtained:

$$\begin{aligned} F(h, S, f_{ck}, \tau, c_t, c_c) &= \bar{F} + c_1^F.\tfrac{(h-\bar{h})}{\sigma_h} + c_2^F.\tfrac{(S-\bar{S})}{\sigma_S} + c_3^F.\tfrac{(f_{ck}-\bar{f_{ck}})}{\sigma_{f_{ck}}} + c_4^F.\tfrac{(\tau-\bar{\tau})}{\sigma_\tau} + c_5^F.\tfrac{(c_t-\bar{c_t})}{\sigma_{c_t}} + c_6^F.\tfrac{(c_c-\bar{c_c})}{\sigma_{c_c}} \\ &= -196.4 + 160.2\tfrac{(h-1.65)}{(2.1-1.65)} + 16.9\tfrac{(S-24.5)}{(37-24.5)} + 23.5\tfrac{(f_{ck}-50)}{(60-50)} \\ &\quad -7.2\tfrac{(\tau-0.1413)}{(0.1571-0.1413)} - 123.2\tfrac{(c_t-0.75)}{(1-0.75)} - 128.7\tfrac{(c_c-0.75)}{(1-0.75)} \end{aligned} \quad (5)$$

$$\begin{aligned} r_{damaged}(h, S, f_{ck}, \tau, c_t, c_c) &= \bar{r}_{damaged} + c_1^{r_{damaged}}.\tfrac{(h-\bar{h})}{\sigma_h} + c_2^{r_{damaged}}.\tfrac{(S-\bar{S})}{\sigma_S} + c_3^{r_{damaged}}.\tfrac{(f_{ck}-\bar{f_{ck}})}{\sigma_{f_{ck}}} \\ &\quad + c_4^{r_{damaged}}.\tfrac{(\tau-\bar{\tau})}{\sigma_\tau} + c_5^{r_{damaged}}.\tfrac{(c_t-\bar{c_t})}{\sigma_{c_t}} + c_6^{r_{damaged}}.\tfrac{(c_c-\bar{c_c})}{\sigma_{c_c}} \\ &= 4565.4 - 2639.9.\tfrac{(h-1.65)}{(2.1-1.65)} + 12.4\tfrac{(S-24.5)}{(37-24.5)} - 217.6\tfrac{(f_{ck}-50)}{(60-50)} \\ &\quad -379.2\tfrac{(\tau-0.1413)}{(0.1571-0.1413)} + 1611.7\tfrac{(c_t-0.75)}{(1-0.75)} + 2124.2\tfrac{(c_c-0.75)}{(1-0.75)} \end{aligned} \quad (6)$$

$$\begin{aligned} R_{force}(h, S, f_{ck}, \tau, c_t, c_c) &= \bar{R}_{force} + c_1^{R_{force}}.\tfrac{(h-\bar{h})}{\sigma_h} + c_2^{R_{force}}.\tfrac{(S-\bar{S})}{\sigma_S} + c_3^{R_{force}}.\tfrac{(f_{ck}-\bar{f_{ck}})}{\sigma_{f_{ck}}} \\ &\quad + c_4^{R_{force}}.\tfrac{(\tau-\bar{\tau})}{\sigma_\tau} + c_5^{R_{force}}.\tfrac{(c_t-\bar{c_t})}{\sigma_{c_t}} + c_6^{R_{force}}.\tfrac{(c_c-\bar{c_c})}{\sigma_{c_c}} \\ &= 123.1 + 3.8\tfrac{(h-1.65)}{(2.1-1.65)} - 2.1\tfrac{(S-24.5)}{(37-24.5)} - 5.3\tfrac{(f_{ck}-50)}{(60-50)} \\ &\quad +0.2\tfrac{(\tau-0.1413)}{(0.1571-0.1413)} - 7.5\tfrac{(c_t-0.75)}{(1-0.75)} - 5.9\tfrac{(c_c-0.75)}{(1-0.75)} \end{aligned} \quad (7)$$

These formulas provide a rapid way to estimate the desired parameter in optimal design without using a finite element calculation. Due to the nonlinearity of the results obtained by the simulation, an error limited here by the range of parameters chosen is induced by these equations. This is especially true and even more important when the applied momentum is away from the initial one. It is therefore recommended to keep c_t and c_c as equal to 1 in order to have a lower error. The error induced for the other parameters is quite limited due to the linear results in the chosen range of variations.

However, this formulation is robust and provides reliable results in the range of variation of the parameters used and so if the impact does not produce the perforation of the structure. To conclude, uncertainty and errors are quite limited in these ranges of parameters but one should deepen this approach and associated statistical errors in order to are them in a more general framework for aircraft impact study on NPP. Here it is important to highlight that this statistical approach was developed to limit the numerical costs.

5. Conclusions and perspectives

In this paper the impact of different geometries and slab boundary conditions were first studied by means of parametric analysis.

We presented a parametric analysis to observe the influence of the different values taken by each chosen parameter. This provided us with essential informations on the simulations – the limit between perforation and bending range for instance. The aim was to place ourselves in a case of shaking of structures that refers to a bending problem. In addition, the perforation case creates various problems outside the scope of continuum theory.

The last step presents the results obtained by performing a reduced sensitivity analysis. For this, we used the Taguchi method taht gave a table for limiting the number of simulations. We then obtained the influence between the different parameters studied. From there, we were able to establish an order of importance for each variable and to propose empirical formulas to estimate roughly the influence of each parameters.

To conclude, this sensitivity study allowed us to realize that it is difficult to identify a direct relationship between inputs and outputs in the case of the simulation of aircraft impact on a civil engineering structure, particularly in terms of nonlinear area and reaction at the boundary of this area. Also the results and formulas obtained are valid for aircraft impact load cases leading to flexural problems. It is thus useful in an optimal design. Outside this range, these formulas are not usable.

References

[1] Babuška, I., Ihlenburg, F., Paik, E. T., and Sauter, S. A. (1995). A generalized finite element method for solving the helmholtz equation in two dimensions with minimal pollution. *Computer Methods in Applied Mechanics and Engineering*, 128(3):325–359.

[2] Bangash, M. (1993). *Impact and explosion: analysis and design.* Blackwell Scientific Publication.

[3] Box, G. E., Hunter, W. G., Hunter, J. S., et al. (1978). Statistics for experimenters.

[4] CEB, editor (1988). *Concrete Structures under Impact and Impulsive Loading, Synthesis Report.* Comité Euro-International du Béton. Bulletin d'information 187.

[5] Chambart, M., Desmorat, R., and Gatuingt, F. (2014). Intrinsic dissipation of a modular anisotropic damage model: application to concrete under impact. *Engineering Fracture Mechanics*, 127:161–180.

[6] de Rocquigny, E., Devictor, N., and Tarantola, S. (2008). *Uncertainty in industrial practice: a guide to quantitative uncertainty management*. John Wiley & Sons.

[7] EC2 (2005). *Eurocode 2 - Calcul des structures en béton*. NF EN 1992-1-1.

[8] Eibl, J. (1987). Soft and hard impact. In *Proceedings of the First International Conference on Concrete for Hazard Protection, Edinburgh*.

[9] Hallquist, J. (2006). *LS-DYNA theory manual*. Livermore Software Technology Corporation.

[10] Hervé, G., Gatuingt, F., and Ibrahimbegovic, A. (2005). On numerical implementation of a coupled rate dependent damage-plasticity constitutive model for concrete in application to high-rate dynamics. *Engineering Computations*, 22(5/6):583–604.

[11] Hervé, G., Rouzaud, C., Barré, F., and Secourgeon, E. (2013). Optimizing the analysis of airplane crash induced spectra by means of generic airplane methodology. In *Proceedings of the 22nd SMiRT, San Francisco, USA*.

[12] Koechlin, P. and Potapov, S. (2009). Classification of soft and hard impacts - application to aircraft crash. *Nuclear Engineering and Design*, 239(4):613–618.

[13] Ladevèze, P., Arnaud, L., Rouch, P., and Blanzé, C. (2001). The variational theory of complex rays for the calculation of medium-frequency vibrations. *Engineering Computations*, 18:193–214.

[14] Ladevèze, P. and Riou, H. (2005). Calculation of medium-frequency vibrations over a wide frequency range. *Computer methods in applied mechanics and engineering*, 194(27):3167–3191.

[15] Lemaitre, J. and Chaboche, J.-L. (1994). *Mechanics of solid materials*. Cambridge university press.

[16] Ls-Dyna (1976). http://www.lstc.com/.

[17] Mazars, J. (1986). A description of micro-and macroscale damage of concrete structures. *Engineering Fracture Mechanics*, 25(5):729–737.

[18] Ragueneau, F., Desmorat, R., and Gatuingt, F. (2008). Anisotropic damage modelling of biaxial behaviour and rupture of concrete structures. *Computers and Concrete*, 5(4):417–434.

[19] Riera, J. D. (1980). A critical reappraisal of nuclear power plant safety against accidental aircraft impact. *Nuclear Engineering and Design*, 57(1):193–206.

[20] Rouzaud, C., Gatuingt, F., Dorival, D., Hervé, G., and Kovalevsky, L. (2015). A new way for the simulation of the impact on reinforced concrete structures. *Engineering Computations*, 32(8):2343–2382.

[21] Snozzi, L., Gatuingt, F., and Molinari, J.-F. (2012). A meso-mechanical model for concrete under dynamic tensile and compressive loading. *International journal of fracture*, 178(1-2):179–194.

[22] Souvay, P. (1994). *Les plans d'expériences, Méthode Taguchi.* AFNOR.

[23] Sugano, T., Tsubota, H., Kasai, Y., Koshika, N., Orui, S., Von Riesemann, W., Bickel, D., and Parks, M. (1993). Full-scale aircraft impact test for evaluation of impact force. *Nuclear Engineering and Design*, 140(3):373–385.

[24] Taguchi, G. (1986). *Introduction to Quality Engineering.* Asian Productivity Organisation.

[25] Taguchi, G. and Konishi, S. (1987). *Orthogonal arrays and linear graphs: tools for quality engineering.* American Supplier Institute Allen Park, MI.